Appearance of vortices in rotating He II

C. A. Jones and K. B. Khan
Department of Mathematics, University of Exeter, Exeter EX4 4QE, United Kingdom

C. F. Barenghi and K. L. Henderson*
Department of Mathematics and Statistics, University of Newcastle upon Tyne, Newcastle upon Tyne NE1 7RU, United Kingdom
(Received 13 December 1994)

The conditions for the appearance and disappearance of quantized vortices in rotating superfluid helium are examined. Our approach is based on the two-fluid model of He II. Using a local-momentum-conservation equation, appropriate when the appearance and disappearance of vortices is on a short time scale compared with normal fluid viscous times, we find that the free-energy theory has to be modified. The new theory predicts hysteresis between increasing and decreasing angular velocity, as observed in some experiments. The theory is applied to some experiments on uniformly rotating superfluid, and also to experiments on Couette flow. Finally, we consider the stability of a vortex row between rotating cylinders to perturbations independent of the direction of the rotation axis.

I. INTRODUCTION

The existence of quantized vortices in superfluid helium II was established over 30 years ago, but the question of how such vortices are created and destroyed is still not well understood. In this paper we consider configurations in which the helium is rotating, but we allow the possibility of nonuniform rotation, so we include the case of general Taylor-Couette flow between rotating cylinders.

Feynman[1] showed that the energy of uniformly rotating helium is minimized if the quantized vortices form an array parallel to the rotation axis (z axis) of density $n=2\Omega/\kappa$ where Ω is the rotation rate and κ is the quantum of circulation, 9.97×10^{-4} cm^2 s^{-1}. In situations where there are many vortices in the apparatus, this Feynman rule is always approximately obeyed. This does not, however, shed much light on the processes by which vortices are created or destroyed so that the Feynman rule state is attained.

Since the vortices are quantized, a complete understanding of the processes of creation and destruction will require a quantum description. This is a substantial undertaking, and is not attempted here; this work is based on a semiclassical hydrodynamic approach. One of our objectives is to discover where semiclassical methods can give agreement with experiments, and where they are inadequate.

The motivation for this work came from recent experiments by Swanson and Donnelly[2] and Bielert and Stamm[3] on helium rotating between concentric cylinders. Swanson and Donnelly[4] (hereafter referred to as SD87) predicted using free-energy arguments that the onset of quantized vortices would occur at a certain value of the Reynolds number $\mathrm{Re}=\mathrm{Re}_0$. Theoretical work by Barenghi and Jones[5] and Barenghi[6] based on the Hall-Vinen-Bekharevich-Khalatnikov (HVBK) equations predicted that at higher $\mathrm{Re}=\mathrm{Re}_1$ a transition would occur in the flow with the onset of toroidal Taylor vortices. The experiments did indeed find critical Reynolds numbers marking the onset of vortices and the Taylor-Couette transition. While the Taylor-Couette transition did occur at approximately the correct value of the Reynolds number, the onset of vortices occurred at a critical Reynolds number two to three times greater than that predicted by SD87. This raised doubts about the validity of the free energy method for determining the rotation rates at which vortices onset in the Taylor-Couette problem, and prompted this investigation.

The mechanisms that we envisage for the creation and destruction of superfluid vortices are (i) spontaneous creation or destruction in the interior of the He II, due to an energetically favorable transfer of momentum between the normal-fluid component and the superfluid component and (ii) creation or destruction of vortices at a boundary. Actually, the second process can destroy vortices, but it cannot create them, except possibly at very high rotation rates, because of the energy barrier that exists near a boundary.[7,8]

Another possibility is that the vortices found in experiments in rotating He II are the result of the stretching of remnant vortices by large-scale meridional flow. Such flows occur in classical fluids when the rotation rate is changed, driven by Ekman pumping in the viscous boundary layer. This process may well be important in some experiments, but in carefully controlled experiments at low rotation rates the vortex states attained have a degree of repeatability which might not be expected if the formation process depended entirely on random initial conditions and weak meridional circulations. We shall not explore this possibility further.

The process of destruction of vorticity at the walls of the container will be enhanced if instabilities occur which drive vortices towards the boundaries. It is well-known that many classical vortex array configurations are unstable. In consequence, even when the formation of such an array is energetically favorable, it may disintegrate if the

array is unstable and the vortices will be lost at the walls. Naively, because of these instabilities it is hard to see how vortex arrays can form at all; however, as we see below, the mutual friction between the superfluid and normal-fluid components can stabilize certain vortex arrays.

The outline of this paper is as follows: in Sec. II we develop the energy criterion for creation and destruction of vortex lines under the semiclassical assumption that the transitions are fast and locally conserve the total momentum of superfluid plus normal fluid components. In Sec. III we apply this theory to experiments of Mathieu, Marechal, and Simon,[8] hereafter referred to as MMS80, in which repeatable hysteresis loops between vortex formation and destruction were obtained. In Sec. IV we apply the theory to the onset of vortices in Couette flow. In Sec. V we examine the stability of vortex arrays to small two-dimensional perturbations independent of z, and finally we draw conclusions as to the successes and limitations of this semiclassical hydrodynamic approach.

II. ENERGY CRITERION FOR THE ONSET OF VORTICES

The principle of minimization of free energy has been widely applied to predict both the appearance of superfluid vortices in rotating systems and the expected final configuration. Some success has been achieved (see, e.g., Donnelly[9]), but some problems remain. The method has proved very successful in predicting final configurations of a given number of vortices,[10] although the existence of a number of local minima in the free-energy function sometimes makes it difficult to be sure that an experiment will always find the absolute minimum configuration. However, the method is not nearly so successful in predicting when vortices appear or disappear. In particular, it is not clear how the free-energy method is to be extended to cases where nonuniform rotation is to be expected, as in Couette flow. Swanson and Donnelly[4] have proposed a criterion for the first appearance of vortices, but recent experiments[2,3] suggest that the actual first appearance of vortices occurs at a rotation rate two to three times faster than their formula predicts.

A further difficulty with the free-energy argument is that it predicts that vortices should disappear as the rotation rate is reduced at the same angular velocity as vortices appear as the angular velocity is increased. It does not predict hysteresis. However, experiments, particularly those at lower temperatures, suggest that such a hysteresis does exist. Packard and Sanders,[11] for example, found a significant difference between the behavior during spin-up and spin-down, with vortices persisting as the angular velocity is decreased well below the value at which vortices appeared as the angular velocity increased.

A more conceptual objection to the free-energy argument is that although the rotation rate of the container explicitly appears in the formula for onset, it is not always entirely clear how what is happening to the container can affect the superfluid. Of course, if a normal-fluid component is present, it will spin up to the angular velocity of the container by viscous action. However, the free-energy argument is independent of the normal-fluid density, suggesting that it should apply even at zero temperature when there is no normal fluid. If the superfluid does not interact with the container and there is no normal fluid, how can the superfluid know that the container is rotating at all? Nevertheless, despite these objections, it is clear from the experiments that there is a connection between free energy and vortex formation, so we now reexamine the conditions for vortex formation, explicitly taking into account the role of the normal fluid and considering possible coupling to the container.

We consider a transition from a state with a given number and distribution of superfluid vortices to a state with a different number and distribution. Since we think of this transition as a single event, the state achieved after the transition will not necessarily be the final state; further transitions or adjustments may occur subsequently. We let the velocity of the normal fluid before the transition be $\mathbf{v}_n$ and the velocity of the normal fluid after the transition be $\tilde{\mathbf{v}}_n$. All velocities refer to an inertial (laboratory) frame, rather than the rotating frame sometimes used in free-energy calculations. Similarly, the velocities of the superfluid component before and after the transition are $\mathbf{v}_s$ and $\tilde{\mathbf{v}}_s$, respectively. The transition will only be possible provided that the energy of the configuration before the transition exceeds the energy after, i.e.,

$$E_n + E_s > \tilde{E}_n + \tilde{E}_s \ , \tag{2.1}$$

where $E_n = \rho_n \int \mathbf{v}_n^2 / 2dv$ and $E_s = \rho_s \int \mathbf{v}_s^2 / 2dv$ are volume integrals over the whole fluid, and $\tilde{E}_n, \tilde{E}_s$ are defined similarly. We shall henceforth assume that if the energy for a transition is available, it will take place.

We assume that the initial state is known, so that we can calculate E_n, and from the proposed transition between superfluid states we can evaluate E_s and $\tilde{E}_s$. Criterion (2.1) will hold whether the transition is fast or slow, but to use it we need to find $\tilde{E}_n$, and this requires some assumptions about the nature of the transition.

The first assumption we make is that the appearance of each individual quantized vortex happens on a very rapid quantum time scale, so that momentum is conserved locally, at each point in the fluid. This time scale can be estimated as $t_{\text{quant}} \sim a^2/\kappa \sim 10^{-13}$ s, where a is the vortex core parameter. We also assume that at the moment of creation, the vortex is not coupled to the walls, so that no angular momentum is transferred to the walls. Immediately after the formation of the vortex, adjustment to the pressure distribution, and hence to the momentum distribution, will occur on the sound speed time scale. Further adjustments will occur on the viscous diffusion time scale. We assume that the quantum time scale is much faster than these effects, so that they do not affect the process of formation, but only what is subsequently observed.

The transitions that involve the creation or destruction of a vortex in the interior of the fluid will then be fast, and local conservation of momentum then implies

$$\rho_n \mathbf{v}_n + \rho_s \mathbf{v}_s = \rho_n \tilde{\mathbf{v}}_n + \rho_s \tilde{\mathbf{v}}_s \ . \tag{2.2}$$

We can now eliminate $\tilde{\mathbf{v}}_n$ from (2.1) using (2.2) to obtain

$$\int \rho_s(\mathbf{v}_s-\mathbf{v}_n)^2 dv > \int \rho_s(\tilde{\mathbf{v}}_s-\mathbf{v}_n)^2 dv + \frac{\rho_s}{\rho_n}\int \rho_s(\tilde{\mathbf{v}}_s-\mathbf{v}_s)^2 dv \quad (2.3)$$

as the necessary and sufficient condition for the transition to occur.

If the normal fluid is initially in a state of uniform rotation, and if ρ_s/ρ_n is small, we can then neglect the second term on the right and the transition will take place provided that

$$E_s-\boldsymbol{\Omega}\cdot\mathbf{L}_s > \tilde{E}_s-\boldsymbol{\Omega}\cdot\tilde{\mathbf{L}}_s \ , \quad (2.4)$$

where $\mathbf{L}_s=\int \rho_s \mathbf{r}\times\mathbf{v}_s dv$ and $\tilde{\mathbf{L}}_s=\int \rho_s \mathbf{r}\times\tilde{\mathbf{v}}_s dv$ is the angular momentum of the superfluid before and after transition. (2.4) is equivalent to saying that the system will minimize the "free energy" $E_s-\boldsymbol{\Omega}\cdot\mathbf{L}_s$, the criterion which has been very extensively used to predict the final state of vortex configurations (see Hall;[12] references and discussion in Donnelly[9]).

However, (2.3) is not equivalent to (2.4) unless $\zeta=\rho_s/\rho_n$ is small, i.e., the temperature is close to the λ-point temperature, T_λ. It is helpful to apply (2.3) to the classic problem of the formation of a single vortex[1] at the center of a cylinder of radius b rotating at angular velocity Ω. If the initial state is one of uniformly rotating normal fluid and stationary superfluid, and we consider a possible transition to a state in which there is a singly quantized superfluid vortex, (2.3) predicts transition provided

$$\Omega > \frac{\kappa}{2\pi b^2}\ln\left[\frac{b}{a}\right](1+\zeta) \ , \quad (2.5)$$

where a is the core parameter, normally $O(10^{-8})$ cm, which differs from the result given by the free-energy argument,

$$\Omega > \Omega_0=\frac{\kappa}{2\pi b^2}\ln\left[\frac{b}{a}\right] \quad (2.6)$$

[e.g., Donnelly,[9] Eq. (2.21)] by the factor $(1+\zeta)$. The physical reason for this difference is that our argument assumes that the momentum gained by the superfluid is lost (locally) by the normal fluid. This is a more restrictive assumption than the free-energy argument which assumes that superfluid momentum can be passed to the container during transition, which is further assumed to have a large moment of inertia (e.g., to be fixed in the rotating frame). Note that the essential difference between (2.5) and (2.6) relies on there being no transfer of angular momentum to the container *during the vortex formation process;* subsequent to the vortex formation, the normal fluid will again come into solid body rotation with the container through the action of normal-fluid viscosity, so that angular momentum will always eventually be transferred to the container, as indeed has been observed in experiments.[13]

Given that we know very little about the quantum processes involved in the transition between different states, it is of interest to consider the results derived from making assumptions other than strict local momentum conservation (2.2). Suppose instead that for the formation of a single vortex in a rotating cylinder the local angular momentum of the superfluid and normal fluid is conserved outside a cylinder of radius c, but that within a radius c only the total angular momentum is conserved. We will assume there is no interaction with the container during transition, but that the normal-fluid velocity after transition is that which gives the minimum critical value of Ω. This might provide a crude model of a situation where the mean free path of excitations is c, and so momentum transfer on the quantum time scale might extend over a distance c rather than being purely local. We then find (assuming $b \gg a$) that the critical value of Ω is

$$\Omega=\frac{\kappa}{2\pi b^2}\left\{\ln\left[\frac{b}{a}\right]+\zeta\left[\frac{c^2-a^2}{c^2+a^2}+\ln\left[\frac{b}{c}\right]\right]\right\} . \quad (2.7)$$

In the limit of exact local momentum conservation, where $c=a$ since the vortex is assumed hollow core, we recover (2.5). In the limit where $c=b$ so that momentum transfer can occur over the whole fluid (but not to the walls) we obtain

$$\Omega=\frac{\kappa}{2\pi b^2}\left\{\ln\left[\frac{b}{a}\right]+\zeta\right\} . \quad (2.8)$$

If coupling to the container is permitted then the ζ term in (2.8) is removed and we have the usual formula (2.6). In most laboratory configurations $\ln(b/a)$ will be in the range 15–20, and the factor ρ_s/ρ_n will be similar at temperature $T\sim 1.4$ K.

The above arguments cannot give a definitive answer to whether (2.5), (2.6), or (2.7) is the more appropriate criterion, and in the absence of a quantum theory of liquid helium the theoretical position is not clear. However, the characteristic time for the diffusion of momentum in the normal fluid in the rotating cylinder is the spin-down time

$$t_{\text{diff}}=(b^2/\nu\Omega)^{1/2} \ ,$$

where ν is the normal-fluid viscosity. This time will be of the order of minutes in a typical experiment; it seems very likely that the time taken to establish the transition from one superfluid vortex state to another will be much less than this, and that (2.2) and (2.5) are generally the most appropriate formulas; we know of no observations which suggest that fractionally quantized vorticity exists in He II even transiently. Nevertheless, it would be interesting to know how fast these transitions take place.

There is some doubt about whether local momentum conservation can be appropriate at very low temperatures, because the mean free path of the excitations which make up the normal fluid increases as the temperature decreases. If the mean free path becomes comparable to the dimensions of the apparatus, it no longer makes sense to use the two-fluid model in the way we are doing. The problem then becomes a much harder one in which the assumption of local thermodynamic equilibrium is no longer valid; we have reached the limit of semiclassical methods and require a quantum approach to resolve this issue.

As mentioned above, the free-energy argument does not predict hysteresis. However, if we use (2.3) to investigate a transition in the rotating cylinder configuration from a superfluid state with a singly quantized vortex on the axis to a state with no superfluid vorticity, we find that as the angular velocity is reduced the central vortex disappears when

$$\Omega < \frac{\kappa}{2\pi b^2}(1-\zeta)\ln\left[\frac{b}{a}\right] . \tag{2.9}$$

Since this differs from (2.5), local conservation of momentum implies the existence of hysteresis. Indeed, according to (2.9) if $\rho_s > \rho_n$, so that $\zeta > 1$, as happens below about 1.95 K, even if the angular velocity is reduced to zero the central superfluid vortex will remain forever.

We now briefly review the experimental evidence to see whether our arguments are consistent with what has already been done. First we note that experimenters have noticed that in order to get results in agreement with the free-energy predictions it is necessary to first establish the rotation of the apparatus and then to lower the temperature below T_λ, rather than to first establish the temperature and then to increase the rotation rate.[14] The above considerations indicate why that should be so; if the rotation rate is held constant as the temperature is lowered below T_λ, the system goes through a state just below T_λ where ρ_s/ρ_n is small, so that (2.1) and (2.2) give the same result as the free-energy argument. Once the vortex (or vortices) has formed just below T_λ, it will remain as the temperature is lowered. On the other hand, if the temperature is first lowered below T_λ, and then the rotation is started up, the angular velocity has to get to the higher value suggested by (2.5), since ρ_s/ρ_n is then never small during the rotation. This suggests that (2.5) [and hence (2.1) and (2.2) on which it is based] bears at least as good a comparison with experiments as (2.6).

Some supporting evidence for (2.5) is found in the experiment of Lynall *et al.*[15] They measured the critical velocity Ω for the appearance of vortices in an annulus as a function of temperature. Their aim was to determine the core parameter a from the free-energy formula (2.6) for Ω_0. Although they failed to reproduce the expected change of a with temperature in the region near T_λ, their data for $T < 2.1$ K are relevant to our discussion because they were taken by first lowering the temperature and then rotating the annulus. In this range Lynall *et al.* discovered a temperature dependence which cannot be explained by (2.6). For example, for an annulus of width $b = 0.0762$ cm, they found that Ω changes by 21.2% from $T = 2.07$ K to $T = 1.97$ K. This large change cannot be taken into account by the weak variation in temperature of the vortex core parameter,[16] for which Ω_0 changes by only 3.9%, but is more consistent with our prediction (2.5) because $1+\zeta$ changes by 21.9%. Similar results were obtained using other values of the width b.

There are however some experiments which are difficult to explain on the basis of (2.5). The first is the result of Packard and Sanders;[11] they found the appearance of the singly quantized vortex in a very small cylinder at 1.2 K to be at 1.6 rad s^{-1} when the free-energy argument predicts 1.0 rad s^{-1}. Because the ratio of ρ_s/ρ_n is so large at this low temperature, (2.5) predicts a much higher critical Ω than 1.6 rad s^{-1}. Apparently, local conservation of momentum does not hold at temperatures this low, otherwise it is hard to see how the vortex could form. Perhaps this is not too surprising, because at this temperature the mean free path of the excitations responsible for the normal fluid is long. In some way, the vortex seen by Packard and Sanders must have formed by a direct coupling between the superfluid and the walls, allowing transfer of angular momentum from superfluid to container on a fast time scale.

The second is the experiment of Swanson and Donnelly,[17] which was cooled first and rotated later. The critical velocity was found to be about 10% lower than predicted by (2.6) at temperatures ranging between 1.5 to 2.165 K, in disagreement with (2.5). A similar percentage lower value was determined by Shenk and Mehl[18] at 1.8, 1.65 and, with some uncertainty, at 1.4 K. A possible explanation is that, as pointed out by Swanson and Donnelly,[19] the amount of mechanical vibrations introduced by the stepping motor was significant and the cell was set in rotation relatively quickly. Swanson and Donnelly and Shenk and Mehl did not observe the hysteresis found by MMS80, who took great care to reduce the noise due to the transmission coupling (servomotor, ball bearings, etc.) and the electronics. Mechanical vibrations are likely to introduce violations of the local law of conservation on which (2.5) is based, and MMS80 report that the effect is very sensitive on the noise level.

Note also that (2.3) does not depend on the normal fluid being initially in a state of uniform rotation, so that it can be applied to situations such as Couette flow with as much validity as when applied to the rotating bucket experiments. However, the criterion (2.3) needs care when being applied, for the appearance or nonappearance of a new state depends now on how it is reached; for example, if we slowly increase the angular velocity in the rotating cylinder, we might find an Ω_1 at which the transition from no vortices to one vortex occurs, and an Ω_2 where the transition from one to two vortices occurs. However, this Ω_2 will not necessarily be the same rotation rate as would be required for a direct transition from no vortices to two vortices.

When comparing results of the free-energy theory with experiment, many authors have used the concept of metastability to explain why their observed states do not correspond to the state of minimum free energy. From our point of view, at a finite temperature below T_λ free-energy theory is invalid when considering transitions which change the number of vortices; however, when considering the final configuration of a fixed number of vortices, our requirement that any change locally conserves momentum no longer applies. There is no reason why an adjustment of the positions of the vortices should take place rapidly, so the momentum constraint is relaxed and free energy should try to minimize. It is however possible that a local minimum rather than a global minimum will be found by the system, and we describe such a state as a metastable state. We prefer to make a sharp distinction between situations where the number of

vortices is constant, in which there is a potential for the system which may give rise to metastability, and situations where the number of vortices is not constant in which there is no potential for the system so that the concept of metastability is inappropriate.

III. APPLICATION TO THE EXPERIMENT OF MATHIEU, MARECHAL, AND SIMON

In the experiment of MMS80, a rectangular cavity 6 mm by 49 mm containing He II was rotated. Superfluid vortices formed, and were detected using the second-sound method. As expected from free-energy theory, the vortices form an array in the interior of the cavity, bordered by a vortex-free strip. At a rotation rate of $\Omega=\Omega_0=1.3\ \mathrm{s}^{-1}$, they showed that the free-energy method predicts a strip of width $d_0=0.25$ mm, with $N_0=6970$ vortices in the cavity. They noted that after any strong perturbation of the system this state was obtained. However, if the velocity was very gradually increased and decreased over a range $\Omega_0-\Delta\Omega<\Omega<\Omega_0+\Delta\Omega$ and the number of vortices N in the cavity was measured, a hysteresis loop was obtained; their experimental data is replotted in Fig. 1. The key observation is that this hysteresis loop, although dependent on the temperature, was reproducible between different experimental runs.

In addition to the experiment, MMS80 also set up a rather elegant mathematical technique for calculating the energy and momentum changes associated with changing vortex distributions, which enables us to approximately evaluate the integrals in (2.3) for this configuration. At $\Omega=\Omega_0$ the extremes of the hysteresis loop correspond to $N=N_1$ and $N=N_2$ vortices, corresponding to a vortex-free strip of width $d=d_1=0.39$ mm and $d=d_2=0.15$ mm, respectively. Our new ideas only affect vortex formation and destruction; for a fixed number of vortices we expect to find the configuration of minimum free energy (ignoring the possibility of metastability in the sense defined in Sec. II), which, as shown by MMS80, consists of an array of vortices at the density $n=2\Omega/\kappa$ given by the Feynman rule surrounded by the vortex-free strip. We interpret the experiments, as did MMS80, as indicating that as the angular velocity is increased along the lower slope of the hysteresis loop the width of the strip is constant at $d=d_1$, and vortices are being added to keep the interior region at the Feynman rule density. When the angular velocity is then reduced down from $\Omega_0+\Delta\Omega$ initially no vortices are lost, but the Feynman rule predicts that the density of vortices must decrease, so the width of the vortex-free strip starts to reduce. This is why there is a flat top to the hysteresis loop. However, when the interior region has expanded so that $d=d_2$, vortices start to disappear, and the system moves down in angular velocity along the upper slope of the hysteresis loop. This continues until the angular velocity is reversed at $\Omega_0-\Delta\Omega$. Then along the flat bottom of the loop the number of vortices is constant but the vortex-free strip widens, until it reaches $d=d_1$ and vortices start coming in again along the lower slope of the loop.

The theoretical points that require explanation are why do new vortices start to enter when d is increased past d_1, and why are vortices lost when d is reduced past d_2? Actually, an explanation of why vortices are lost when $d=d_2$ was given by MMS80, and we believe their reasoning was correct; the free-energy barrier at the walls disappears at approximately $d=0.11$ mm in reasonable agreement with the observed value $d=d_2=0.15$ mm. As they remark, their calculation assumes that the disappearance of the vortices leaves the interior continuum undisturbed, so one would not expect exact agreement. The disappearance of this energy barrier allows vortices to pass across the vortex-free strip to be absorbed at the walls.

They pointed out that vortices could not come in from the walls, because the barrier against the entry of the first vortex is very large (see their Fig. 6); if the mechanism of vortex entry was that creation occurred at the walls and vortices passed across the vortex-free strip into the interior, the process could never get started. The vortices that enter at $d=d_1$ must therefore do so in the interior through the mechanism outlined in Sec. II.

We make the same approximation as MMS80, that the N-vortex configuration in the interior is unperturbed by the addition of a new vortex at a distance y from the wall $y=0$. The superfluid velocity before transition $\mathbf{v}_s$ is that produced by the N vortices in the interior, and the superfluid velocity after transition, $\bar{\mathbf{v}}_s$ corresponds to $\mathbf{v}_s$ with an additional vortex at $\mathbf{r}=(0,y)$. We let $\mathbf{v}_s=\mathbf{v}_{s1}+\mathbf{v}_{s2}$, where $\mathbf{v}_{s1}$ corresponds to the irrotational part of the flow with perpendicular velocity equal to that at the boundaries, and $\mathbf{v}_{s2}$ corresponds to the flow induced by the vortices and their images. Corresponding to $\mathbf{v}_{s2}$ we have a stream function ψ_2 such that $\mathbf{v}_{s2}=\hat{\mathbf{z}}\times\nabla\psi_2$, and $\psi_2=0$ on the boundary. We adopt a similar decomposition for $\bar{\mathbf{v}}_s$. The normal-fluid velocity before transition is $\mathbf{v}_n=\boldsymbol{\Omega}\times\mathbf{r}$. From MMS80,

$$\frac{1}{2}\rho_s\int[\mathbf{v}_s^2-\bar{\mathbf{v}}_s^2]dS=\frac{1}{2}\rho_s\int[\mathbf{v}_{s2}^2-\bar{\mathbf{v}}_{s2}^2]dS \tag{3.1}$$

(the integral being over the whole cavity), because the total energy is the direct sum of the rotational and irrotational parts of the flow. Now

$$\frac{1}{2}\rho_s\int\mathbf{v}_s^2dS=\frac{1}{2}\rho_s\int_{C_i}\psi_2\frac{\partial\psi_2}{\partial n}dl=-\sum_{i=1}^{N}\frac{1}{2}\rho_s\kappa\psi_2(\mathbf{r}_i)\ , \tag{3.2}$$

where $\mathbf{r}_i$ is the location of the ith vortex, and C_i is a contour of radius a around each vortex. When evaluating the energy, we take a as the healing length appropriate for a hollow core vortex,

$$\psi_2(\mathbf{r}_i)=\sum_{i\neq j}\kappa G(\mathbf{r}_j,\mathbf{r}_i)\ , \tag{3.3}$$

where $G(\mathbf{r},\mathbf{r}_i)=g(\mathbf{r},\mathbf{r}_i)+\ln|\mathbf{r}-\mathbf{r}_i|/2\pi$ is the Green's-function solution of

$$\nabla^2G=\delta(\mathbf{r}-\mathbf{r}_i)$$

vanishing on the boundary. Writing similar equations for $\bar{\mathbf{v}}_s$, but summing over $N+1$ to include the extra vortex, we obtain

$$\frac{1}{2}\rho_s \int [\mathbf{v}_s^2 - \bar{\mathbf{v}}_s^2] dS = \rho_s \kappa \psi_2(\mathbf{r}) + \frac{\rho_s \kappa^2}{2}\left[g(\mathbf{r},\mathbf{r}) + \frac{1}{2\pi}\ln a \right] . \tag{3.4}$$

We must also calculate

$$\int \rho_s \mathbf{v}_n \cdot (\bar{\mathbf{v}}_s - \mathbf{v}_s) dS = \rho_s \Omega \int (\mathbf{r}\cdot\nabla)\Psi dS = 2\rho_s \Omega \int \Psi ds , \tag{3.5}$$

where $\Psi = \tilde{\psi}_2 - \psi_2$ is the streamfunction due to the single additional vortex at $\mathbf{r}$. Finally we need

$$\begin{aligned} \zeta \int \frac{1}{2}\rho_s (\bar{\mathbf{v}}_s - \mathbf{v}_s)^2 dS &= \frac{1}{2}\zeta \rho_s \int_C \Psi \frac{\partial \Psi}{\partial n} dl \\ &= -\frac{1}{2}\zeta \rho_s \kappa \Psi(\mathbf{r}) \\ &= -\frac{1}{2}\zeta \rho_s \kappa^2 \left[g(\mathbf{r},\mathbf{r}) + \frac{1}{2\pi}\ln a \right] . \end{aligned} \tag{3.6}$$

To evaluate the required quantities explicitly we adopt the further approximation that the cavity has infinite extent in the x direction, the walls being $y = 0$ and $y = l$. In the appendix of MMS80 it is then shown that if the width of the vortex-free strip is d, then

$$\psi_2 = -\Omega(l - 2d)y , \tag{3.7}$$

and if y and d are small compared to l then

$$g(\mathbf{r},\mathbf{r}) = -\frac{1}{2\pi}\ln[2y] , \quad \int \Psi dS = \frac{1}{2}y(y - l) . \tag{3.8}$$

Substituting these expressions into (3.4), (3.5), and (3.6), and using the criterion for transition (2.3), we see that the transition to the extra vortex state is allowed if

$$\kappa \rho_s \Omega y(2d - y) - \frac{(1+\zeta)\rho_s \kappa^2}{4\pi}\ln(2y/a) > 0 , \quad 0 < y < d . \tag{3.9}$$

Note that as in the MMS80 calculation the criterion does not depend on l, the distance between the walls. The criterion is essentially a local one, dependent only on conditions in the vortex-free strip. Inserting the numerical values appropriate to the MMS80 experiment, $\Omega_0 = 1.3$ s^{-1}, $\zeta = 1.3$ at 1.9 K, and $a = 10^{-7}$ cm and looking for the smallest value of d which allows (3.9), we find that the criterion (3.9) is first satisfied at $d = 0.44$ mm with y then 0.42 mm. The close proximity of y to d is slightly unfortunate, because the addition of the new vortex that close to the interior vortices will disturb the interior vortex configuration, at least for those vortices close to the point where the new vortex enters. Nevertheless, the observed value of $d_1 = 0.39$ mm is in reasonable agreement with our predicted value of 0.44 mm. The experimental and theoretically predicted curves of N against Ω are shown in Fig. 1. The theoretically predicted hysteresis loop is constructed by finding $N_2 = N_0 + 2(d_0 - d_2)L(2\Omega_0/\kappa)$ where $L = 4.9$ cm, $N_0 = 6970$, and $\Omega_0 = 1.3$ s^{-1} in the MMS80 apparatus, and

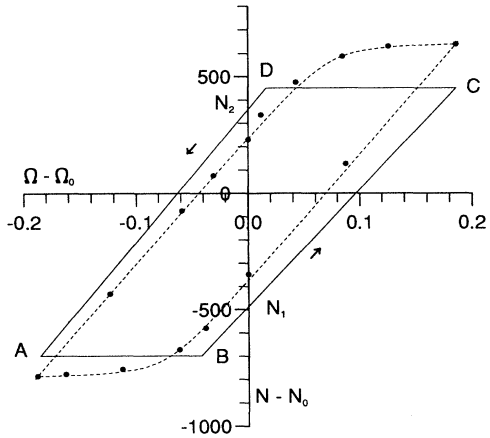

FIG. 1. The number of vortex lines $N - N_0$ as a function of angular velocity $\Omega - \Omega_0$, showing that the number of vortices depends on whether the angular is being slowly increased (lower branch) or decreased (upper branch). In the MMS80 experiment $N_0 = 6970$ and $\Omega_0 = 1.3$ s^{-1}. The points are the experiments, the dashed line being to guide the eye. The solid line is the theoretically predicted hysteresis loop.

$$N_1 = N_0 - 2(d_1 - d_0)L(2\Omega_0/\kappa) .$$

The gradient of the hysteresis loop $dN/d\Omega$ on the upper branch is given by $2L(l - 2d_2)/\kappa$ and on the lower branch by $2L(l - 2d_1)/\kappa$ where $l = 0.6$ cm. The extremities of the loop are given by the experimental value $\Delta\Omega = 0.186$ s^{-1}; this data enables the points labeled A, B, C, and D on Fig. 1 to be found, and the loop to be constructed. Considering that the approximation of ignoring changes of configuration of the interior vortices has been made, the agreement between theory and the experimental values seems quite satisfactory.

The change in the free-energy between the states with and without the vortex is given by MMS80 Eq. (A7) as

$$\Delta F(\mathbf{r}) = \frac{\rho_s \kappa^2}{4\pi}\ln(2y/a) - \kappa \rho_s \Omega y(2d - y) . \tag{3.10}$$

As we would expect, if $\zeta = 0$ then $\Delta F < 0$ is equivalent to (3.9). For values of $d > d_2 = 0.11$ mm, ΔF has a local maximum in the vortex-free strip, so that it is then not advantageous for a vortex to move out from the interior vortex array to the boundary. However, if $d < d_2 = 0.11$ mm the maximum disappears, and it is then favorable for a vortex to move out of the interior array towards the wall, where it is destroyed.

One further point has been revealed by the comparison of this experiment with our theory; if the system is given a strong perturbation, MMS80 found that the system returned to the free-energy equilibrium state of N_0 vortices at Ω_0. We note that our extra factor of $(1+\zeta)$ arises because of the extra constraint of local momentum conservation. If that constraint is removed, for example by jarring the cryostat or momentarily feeding a large dc heat flux into the cavity, hence allowing an external momentum source into the system, the system returns to the minimum free-energy state.

IV. APPLICATION TO COUETTE FLOW

We now apply our theory to the problem of the Couette flow of helium between rotating concentric cylinders. We only examine the case where the outer cylinder is at rest, although the extension to general rotations is straightforward. The main reference here is to Swanson and Donnelly[4] (SD87). The normal-fluid velocity

$$\mathbf{v}_n=(Ar+B/r)\hat{\boldsymbol{\phi}}\ , \tag{4.1}$$

where $\hat{\phi}$ is the unit vector in the azimuthal direction and $A=-\Omega R_1^2/(R_2^2-R_1^2)$ and $B=-AR_2^2$, R_1 and R_2 being the radii of the inner and outer cylinders, respectively. As pointed out by SD87, as the rotation rate of the inner cylinder Ω is gradually increased, the first transitions are not from vortices entering the gap between the cylinders but from virtual vortices arising at the axis building up the irrotational flow of superfluid in the helium. These are however, undetectable by the second-sound technique, since no real vortices enter the gap until the angular velocity Ω is much larger. Applying condition (2.3) to find the value of Ω at which the transition from the state of n virtual vortices to the state of $n+1$ virtual vortices occurs we obtain

$$\begin{aligned}\pi\rho_s\int_{R_1}^{R_2}\left[\frac{n\kappa}{2\pi r}-\frac{B}{r}-Ar\right]^2 r\,dr \\ >\pi\rho_s\int_{R_1}^{R_2}\left[\left[\frac{(n+1)\kappa}{2\pi r}-\frac{B}{r}-Ar\right]^2\right. \\ \left.+\zeta\left[\frac{\kappa}{2\pi r}\right]^2\right]r\,dr\ ,\end{aligned} \tag{4.2}$$

which reduces to

$$\begin{aligned}\left[B-\frac{(2n+1)\kappa}{4\pi}\right]\ln(R_2/R_1)+\frac{A}{2}(R_2^2-R_1^2) \\ >\frac{\zeta\kappa}{4\pi}\ln(R_2/R_1)\ .\end{aligned} \tag{4.3}$$

If the gap $d=R_2-R_1$ between the cylinders is small compared to the radii of the cylinders (normally the case in these experiments), we can expand in powers of d/R_2 to obtain

$$\Omega_n=\frac{(n-1/2+\zeta/2)\kappa}{2\pi}[1+5d/3R_2+O((d/R_2)^2)] \tag{4.4}$$

and the transition from the n to the $n+1$ state occurs when $\Omega>\Omega_n$ as Ω is increased. The strength of the virtual vortex at the origin is $\Gamma_0=n\kappa$ where

$$\Gamma_0=\Omega_n\pi R_2^2[1-5d/3R_2+O((d/R_2)^2)]-\frac{(\zeta-1)\kappa}{2}\ . \tag{4.5}$$

Now we examine the transition where vortices enter the gap. The angular velocity is Ω and since the number of virtual vortices at the origin is large, the vortex strength at the origin, Γ_0, is given by (4.5) with Ω_n replaced by Ω to sufficient accuracy. Before the transition the normal-fluid velocity is given by (4.1) and the superfluid velocity is given by

$$\mathbf{v}_s=\frac{\Gamma_0}{2\pi r}\hat{\boldsymbol{\phi}}\ . \tag{4.6}$$

After the transition the superfluid velocity field has l vortices equally spaced on a circle of radius $(R_1+R_2)/2$ (that this is the optimum position for the vortices was demonstrated by Fetter,[20] hereafter referred to as F67), and the irrotational part of the flow is given by (4.6) but with Γ_0 replaced by an as yet unknown constant Γ_1. Criterion (2.3) can be written

$$E_0>E_1-E_2+E_3\ , \tag{4.7}$$

where

$$\begin{aligned}E_0=\int\frac{1}{2}\rho_s(\mathbf{v}_s^2-2\mathbf{v}_s\cdot\mathbf{v}_n)dv\ ,\quad E_1=\int\frac{1}{2}\rho_s\bar{\mathbf{v}}_s^2dv\ , \\ E_2=\int\rho_s\bar{\mathbf{v}}_s\cdot\mathbf{v}_n dv\ ,\quad E_3=\zeta\int\frac{1}{2}\rho_s(\bar{\mathbf{v}}_s-\mathbf{v}_s)^2dv\ .\end{aligned} \tag{4.8}$$

We need some results which are fortunately easily obtainable from F67;

$$\begin{aligned}E_1=\frac{\rho_s}{4\pi}\ln(R_2/R_2)\left[\Gamma_1-\frac{1}{2}l\kappa\right]^2 \\ +\frac{\rho_s\kappa^2 l}{4\pi}[\ln(2d/\pi a)+1/4]\end{aligned} \tag{4.9}$$

comes from formula (32) of F67 taking the narrow gap limit and locating the vortices midway between the gap. The other quantities we need only require the azimuthally integrated ϕ component of the superfluid velocity $\bar{\mathbf{v}}_s$, which is just the circulation around a circle of radius r; this is easily found from Kelvin's circulation theorem, the result being formula (17) of F67,

$$\int_0^{2\pi}r\bar{v}_\phi d\phi=\Gamma_1+l\kappa\eta(r-r_c)\ , \tag{4.10}$$

where $r_c=(R_1+R_2)/2$ and $\eta(x)=(1+x/|x|)/2$ is the step function. We obtain

$$\begin{aligned}E_2=\rho_s\Gamma_1[Adr_c+B\ln(R_2/R_1)] \\ -\kappa l\rho_s\left[\frac{A(R_2+r_c)d}{2}-B\ln(R_2/r_c)\right]\end{aligned} \tag{4.11}$$

and

$$\begin{aligned}E_3=\frac{\zeta\rho_s}{4\pi}\{\ln(R_2/R_1)[(\Gamma_1-\Gamma_0)^2-l\kappa(\Gamma_1-l\kappa/4)] \\ +2\Gamma_0\kappa l\ln(R_2/r_c)+\kappa^2 l[\ln(2d/\pi a)+1/4]\}\ .\end{aligned} \tag{4.12}$$

We now find the value of Γ_1 that minimizes $E_1-E_2+E_3$, which gives

$$\Gamma_1=\Gamma_0+\frac{l\kappa}{2}+\frac{(\zeta-1)\kappa}{2(\zeta+1)}\ . \tag{4.13}$$

Inserting (4.13) into (4.9), (4.11), and (4.12), and then put-

ting these into (4.7), gives the required criterion. Expanding in powers of d/R_2 the criterion for transition becomes

$$\Omega > \frac{2(1+\zeta)\kappa}{\pi R_2 d}[\ln(2d/\pi a)+1/4]=\Omega_0(1+\zeta)\ , \quad (4.14)$$

which is the criterion derived by SD87 except for the factor $1+\zeta$ on the right-hand side. In Fig. 2 Ω/Ω_0 is plotted as a function of temperature. Also shown are the points from the data sets of Swanson[2] and Bielert and Stamm[3] also plotted in units of Ω_0. The SD87 results are well below the experimental data. For higher temperatures, our theory is an improvement, but is still somewhat below the data points. Below around 1.8 K our results predict Ω much too high and the SD87 theory gives a result much too low. One possibility is that the vortex configuration at onset has a more complicated geometry than a simple ring of vortices midway between the cylinders. Another possibility is that our results are inappropriate at low temperatures because of the problem of the mean free path of excitations no longer being small.

Finally it must be remarked that our theory neglects the possible existence of remnant vortex lines created when cooling through the λ point.[21] These lines may remain attached to the cylindrical walls, may affect the transfer of angular momentum and may interfere with the generation of the first row of vortices via a vortex mill process.[9] Schwarz[22] estimated the velocity of depinning a vortex line from a small bump of radius r_0 as $v_{\rm dep}=\kappa/(2\pi D)\ln(r_0/a)$ where D is the channel size. Using the values $D=b=1$ mm and $r_0\simeq 0.0015$ cm reported by Bielert and Stamm, we find $v_{\rm dep}\approx 0.02$ cm sec^{-1} which is smaller than $\Omega_0 R_1\approx 0.1$ cm sec^{-1}. This suggests that our assumption is justified.

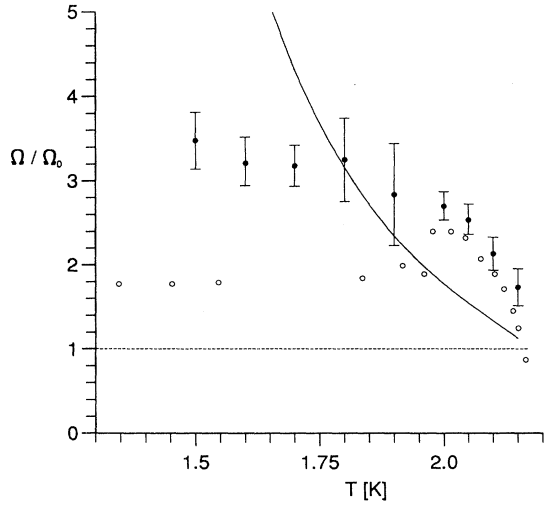

FIG. 2. The angular velocity at the first appearance of vortices as a function of temperature. The angular velocity is plotted in units of $\Omega_0=(2\kappa/\pi R_2 d)[\ln(2d/\pi a)+1/4]$ so that the dashed line corresponds to the SD87 theoretical value. Filled circles with error bars: data of Bielert and Stamm (Ref. 3). Open circles: data of Swanson (Ref. 2). Solid line is prediction of this theory, $1+\zeta$.

V. STABILITY OF VORTEX ROWS

The above considerations can give us information about whether a vortex array can form, but it may be that such arrays are unstable and break up after formation. Indeed, the classical theory of the stability of vortex arrays[23] tells us that most configurations are indeed unstable. Here we investigate the stability of a vortex row in a narrow gap, relevant to the problems studied in F67 and in the Couette flow experiments.

We consider an array of vortices between parallel plates at $y=-d/2$ and $y=d/2$. This approximates the situation of vortices between concentric cylinders provided the gap is narrow compared to the radius. We assume that the vortices are initially in a row at $y=0$ a distance l apart (we depart from Fetter's notation, so that here l is no longer the number of vortices in the gap). If the normal fluid is in a state of uniform shear with vorticity ω

$$\mathbf{v}_n=-\omega y\hat{\mathbf{x}}\ . \quad (5.1)$$

We assume that the vortices remain line vortices, so that we are only considering disturbances independent of the z coordinate. There are two forces acting on a vortex in this flow: a Magnus force $\mathbf{f}_M$ due to the motion of the superfluid around it, and a force $\mathbf{f}_D$ which is the sum of the Magnus force induced by the motion of the normal fluid and the drag caused by the mutual friction between the normal and superfluid components.[9] We neglect the inertia of the vortex lines, so that

$$\mathbf{f}_M+\mathbf{f}_D=\rho_s\kappa(\mathbf{v}_s-\mathbf{v}_L)\times\hat{\mathbf{z}}-\gamma_0\hat{\mathbf{z}}\times[\hat{\mathbf{z}}\times(\mathbf{v}_n-\mathbf{v}_L)] +\gamma_0'\hat{\mathbf{z}}\times(\mathbf{v}_n-\mathbf{v}_L)=0\ , \quad (5.2)$$

where ρ_s is the superfluid density, γ_0 and γ_0' are the mutual friction parameters and $\mathbf{v}_L$ is the velocity of the line vortex itself. The mutual friction parameters are tabulated in Barenghi, Donnelly, and Vinen.[16] If the position of a vortex is at (x_0,y_0), (5.2) gives

$$\gamma_0\dot{x}_0+\dot{y}_0(\rho_s\kappa-\gamma_0')=\rho_s\kappa v_{sy}-\gamma_0\omega y_0\ , \quad (5.3a)$$

$$\dot{x}_0(\gamma_0'-\rho_s\kappa)+\dot{y}_0\gamma_0=-\rho_s\kappa v_{sx}-\gamma_0'\omega y_0\ , \quad (5.3b)$$

where $\mathbf{v}_s$ is the velocity induced at (x_0,y_0) by all the other vortices and their images. The vortices are initially located at $(ml,0)$, m running over all integers, the images of strength κ are initially located at $(ml,2nd)$, and those of strength $-\kappa$ are at $[ml,(2n+1)d]$. To investigate stability, we give the $(m,0)$ vortex a perturbation (x_m,y_m) so that the two sets of image vortices move to $(ml+x_m,2nd+y_m)$ and $[ml+x_m,(2n+1)d-y_m]$, respectively. We assume small perturbations of the form

$$x_m=\alpha_0\exp(\lambda t+im\phi)\ , \quad y_m=\beta_0\exp(\lambda t+im\phi)\ , \quad (5.4)$$

where ϕ is a constant which we can choose without loss of generality to satisfy $0\le\phi\le 2\pi$. Inserting (5.4) into (5.3) and linearizing, we find that the condition for nontrivial solutions is that

$$\lambda^2[\gamma_0^2+(\rho_s\kappa-\gamma_0')^2]+\gamma_0\rho_s\kappa\lambda[C_1-C_2+\omega] -\rho_s\kappa C_2(\rho_s\kappa C_1+\gamma_0'\omega)=0\ . \quad (5.5)$$

The constants C_1 and C_2 appearing in this formula are given by double sums running over the integers m and n, arising from the fact that there is a doubly infinite array of image vortices. Furthermore, these double sums converge slowly so that direct numerical evaluation is not feasible. Fortunately, however, it turns out that all the sums over n required can be evaluated using residues. We thus obtain expressions for C_1 and C_2 involving only sums over all positive integers m,

$$C_1=\frac{\pi\kappa}{d^2}\left[\sum_{m=1}^{\infty}\operatorname{cosech}\frac{\pi ml}{d}\left[\cos m\phi\operatorname{cosech}\frac{\pi ml}{d}-\coth\frac{\pi ml}{d}\right]-\frac{1}{4}\right] \tag{5.6a}$$

and

$$C_2=\frac{\pi\kappa}{d^2}\left[\sum_{m=1}^{\infty}(\cos m\phi-1)\operatorname{cosech}\frac{\pi ml}{d}\coth\frac{\pi ml}{d}\right]. \tag{5.6b}$$

These sums over m converge very rapidly, and hence can be easily evaluated numerically. For stability, we require that the roots of (5.5) should have negative real parts. To analyze this, we first look at the case where there is no coupling to the normal fluid, obtained by setting the mutual friction parameters γ_0 and γ_0' to zero. For stability we then require $C_1C_2\le 0$. Now all the terms in the sums appearing in C_1 and C_2 are negative, so that the product C_1C_2 is necessarily positive, equality only occurring as $l\to\infty$, the case where a single vortex is left in the channel. We deduce that in ideal fluid with no coupling, the vortex array is always unstable.

We can now consider the criterion for the normal fluid to stabilize the vortex row, bearing in mind that for all wave numbers ϕ and ratios l/d, $C_1\le -1/4$ and $C_2\le 0$. The two conditions that must be satisfied are

$$C_1-C_2+\omega\ge 0 \tag{5.7a}$$

and

$$\rho_s\kappa C_1+\gamma_0'\omega\ge 0\ , \tag{5.7b}$$

so the results are actually independent of the coefficient γ_0. Since $C_1\le -1/4$, from (5.7a) the normal fluid can only stabilize the vortex row if the coefficient γ_0' is large enough, i.e., the coupling to the normal fluid is sufficiently strong. The value of ω, the normal-fluid vorticity, must also be large enough for the restoring force provided by the normal fluid to overcome the vortex row instability. The ratio $\gamma_0'/\rho_s\kappa$ is quite small unless we are close to T_λ, so when the vorticity ω is large enough to satisfy (5.7b), (5.7a) is easily satisfied. The inequality (5.7b) is therefore the controlling inequality except very close to T_λ. Furthermore, the first configuration to be stabilized for all ϕ is that where $l\gg d$, i.e., the vortices in the row are well spaced out. In this limit, $C_1\sim -0.25$, so we can easily construct the stability boundary for ω provided we have tables of ρ_s and γ_0' as a function of temperature. In Fig. 3(a) we apply (5.7b) with $C_1=-0.25$ to the Bielert and Stamm[3] experiment; $\omega=\Omega R_1/d$, so the critical value of Ω is given by

$$\Omega=\frac{\rho_s\pi\kappa^2}{4\gamma_0' dR_1}\ , \tag{5.8}$$

where Ω is the rotation rate of the inner cylinder, $R_1=2.9$ cm is the inner cylinder radius and $d=0.1$ cm is the gap width. In Fig. 3(a), we plot the stability boundary of the angular rotation rate Ω of the inner cylinder as a function of temperature for the apparatus of Bielert and Stamm; their data points are given for comparison. We see that the vortex row is unstable at the data points below about 1.8 K, but stable above. The equivalent Fig.

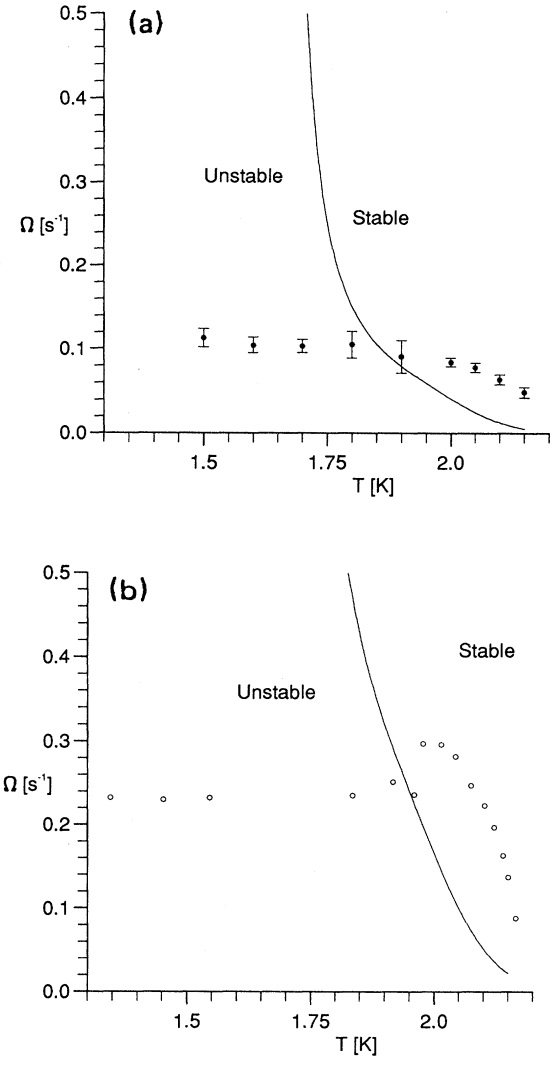

FIG. 3. (a) The stability boundary for a row of vortices for the narrow gap limit. The curve is evaluated for the experimental configuration of Bielert and Stamm (Ref. 3), and their data points are plotted for comparison. This stability curve is determined by the $l/d\to\infty$ limit. (b) As for (a), but evaluated for the experimental configuration of Swanson (Ref. 2), with the data points plotted for comparison.

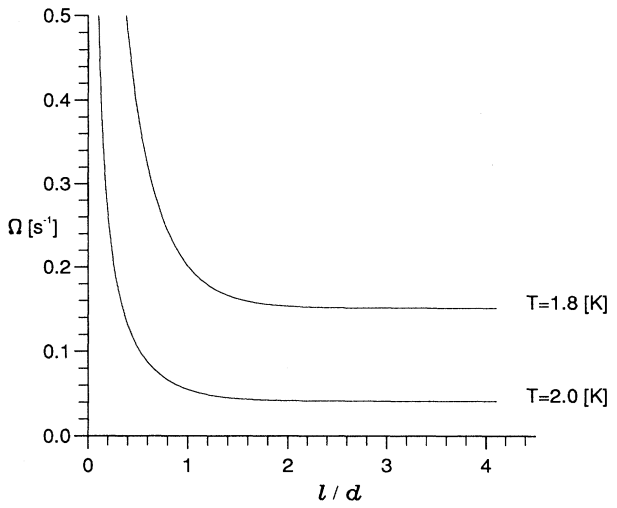

FIG. 4. The stability boundary for a row of vortices for the narrow gap limit as a function of vortex spacing ratio l/d. The curves for $T=1.8$ K and $T=2.0$ K are shown. The curves are evaluated for the experimental configuration of Bielert and Stamm (Ref. 3).

3(b) is plotted for the Swanson[2] data. It is interesting to note that the temperature below which the vortex row becomes unstable marks some anomalous behavior in the Swanson data [Fig. 3(b)], and coincides with the temperature at which the Bielert and Stamm data had rather large error bars [Fig. 3(a)]. This could therefore mark a transition point: the data in both experiments on the right of the stability boundary may correspond to situations where the vortices form a simple row in the middle of the gap, but at lower temperatures, some other (possibly more complex) distribution of vortices may occur.

In Fig. 4 we plot the stability boundary of Ω against l/d at two fixed temperatures; this illustrates how the vortex row is more likely to be unstable if the vortices are closer together. This is what we would expect, since the ideal vortex instability is enhanced by interactions between neighboring vortices. However, we note from this figure that even with the spacing $l/d=1$ the stability boundary is not that different from the $l\rightarrow\infty$ limit.

The main result of this stability analysis is that we expect a row of vortices to be stable at temperatures greater than 1.85 K but to be unstable below that temperature. We have, of course, only considered two-dimensional perturbations independent of the coordinate parallel to the rotation axis. The question then arises, what is the configuration of vortices found in the experiments at temperatures below 1.85 K? There are two possibilities: either the single row configuration is stabilized by end effects (possible pinning of the vortex lines to the end walls), or the first configuration to appear is not in fact a single row of vortices but a double row arranged as in a Kármán vortex street. In an infinite domain, this arrangement of vortices is stable; whether this remains the case when the vortices are confined between walls will require further analysis. It appears reasonable that this configuration will be easier for the normal fluid to stabilize than the single row.

VI. CONCLUSIONS

The free-energy theory has proved a very useful tool in predicting vortex configurations. However, it does have some limitations. The possibility that a vortex system will find a local minimum rather than the global free-energy minimum (the metastability phenomenon) has been realized for some time. In this paper we have drawn attention to the extra constraint coming from local momentum conservation that must be applied when vortex creation or destruction occurs. This can lead to the hysteresis observed in some experiments between increasing and decreasing rotation rate. The revised criterion for the formation of vortices has an extra factor $1+\zeta=1+\rho_s/\rho_n$ over the formula derived by free-energy methods. For temperatures in the range 1.85 K $<T<T_\lambda$ this seems generally to give better agreement with experiments. The agreement obtained with MMS80 hysteresis experiments is encouraging, and the Taylor-Couette experiments become somewhat more comprehensible. At temperatures below 1.85 K the theory does not work well. A number of explanations for this breakdown are possible: the simplest is that at low temperatures the mean free path of the excitations is too large for the normal component to act as a fluid, i.e., the two-fluid model breaks down and a quantum description is required. An alternative explanation might be that the geometry of the vortex formation is more complicated, so that initially vortices are not formed entirely parallel to the rotation axis but are instead attached to the rotating walls. If the vortices are pinned at the walls, this could break the momentum constraint.

Two processes of vortex destruction are indicated. At temperatures below 2 K, the loss of a vortex line in the interior of the fluid can be energetically favorable, because the factor $1-\zeta=1-\rho_s/\rho_n$ can be positive. At slightly lower temperatures, as in the MMS80 experiment, vortices can be pushed into the walls. It is not clear that this mechanism can work when there are only a small number of vortices, because of the energy barrier against an isolated vortex at a wall. At still lower temperatures the breakdown of the two-fluid model may alleviate the local momentum conservation constraint and make it easier for the system to lose vortices.

In addition to considering the energy and momentum conditions on vortex formation and destruction, we have also considered the stability for simple vortex configurations on the two-fluid model. These indicate that in some circumstances the energetically preferred configuration for formation is actually unstable. After formation the vortex pattern must therefore readjust itself. Further work is needed to determine whether more complex arrangements such as the Kármán vortex street configuration are produced in these circumstances.

Finally, we note that it is unlikely that a complete pic-

ture of vortex formation and destruction can be obtained from hydrodynamic models alone. A more fundamental quantum approach is required, especially at low temperatures. The most promising way forward seems to us to be through the condensate model for superfluid helium.

ACKNOWLEDGMENTS

K.B.K. acknowledges support from the Nuffield foundation, and C.F.B, K.L.H., and C.A.J. acknowledge support from EPSRC.

*Present address: Department of Mathematics, University of Bristol, Bristol BS8 1TR, UK.

[1]R. P. Feynman, in *Progress in Low Temperature Physics 1,* edited by C. J. Gorter (North-Holland, Amsterdam, 1955), Chap. 2.

[2]C. J. Swanson and R. J. Donnelly, Phys. Rev. Lett. **67**, 1578 (1991); C. J. Swanson, Ph.D. thesis, University of Oregon, 1991.

[3]F. Bielert and G. Stamm, Physica B **194**, 561 (1994); F. Bielert and G. Stamm, Phys. Fluids **6**, 2826 (1994).

[4]C. E. Swanson and R. J. Donnelly, J. Low Temp. Phys. **67**, 185 (1987).

[5]C. F. Barenghi and C. A. Jones, J. Fluid Mech. **197**, 551 (1988).

[6]C. F. Barenghi, Phys. Rev. B **45**, 2290 (1992).

[7]S. J. Putterman, *Superfluid Hydrodynamics* (North-Holland, Amsterdam, 1974).

[8]P. Mathieu, J. C. Marechal, and Y. Simon, Phys. Rev. B **22**, 4293 (1980).

[9]R. J. Donnelly, *Quantized Vortices in Helium II* (Cambridge University Press, Cambridge, 1991).

[10]L. J. Campbell and R. M. Ziff, Phys. Rev. B **20**, 1886 (1979).

[11]R. M. Packard and T. M. Sanders, Phys. Rev. A **6**, 799 (1972).

[12]H. E. Hall, Philos. Mag. Suppl. **9**, 89 (1960).

[13]G. B. Hess and W. M. Fairbank, Phys. Rev. Lett. **19**, 216 (1967).

[14]K. DeConde and R. E. Packard, Phys. Rev. Lett. **35**, 732 (1975).

[15]I. H. Lynall, D. S. Shenk, R. J. Miller, and J. B. Mehl, Phys. Rev. Lett. **39**, 470 (1977).

[16]C. F. Barenghi, R. J. Donnelly, and W. F. Vinen, J. Low Temp. Phys. **32**, 189 (1983).

[17]C. J. Swanson and R. J. Donnelly, J. Low Temp. Phys. **91**, 81 (1983).

[18]D. S. Shenk and J. B. Mehl, Phys. Rev. Lett. **27**, 1703 (1971).

[19]C. J. Swanson and R. J. Donnelly (private communication).

[20]A. L. Fetter, Phys. Rev. **153**, 285 (1967).

[21]D. D. Awschalom and K. W. Schwarz, Phys. Rev. Lett. **52**, 49 (1984); Y. B. You, Ph.D. thesis, University of Oregon, 1993.

[22]K. W. Schwarz, Phys. Rev. Lett. **47**, 251 (1981); Phys. Rev. B **31**, 5782 (1985).

[23]H. Lamb, *Hydrodynamics* (Cambridge University Press, Cambridge, 1932).